


# Synthesis and Properties of Photodegradable Poly(furan-amine)s by a Catalyst-free Multicomponent Cyclopolymerization

Wei-Qiang Fu, Gui-Nan Zhu, Jian-Bing Shi\*, Bin Tong, Zheng-Xu Cai, and Yu-Ping Dong\*

Beijing Key Laboratory of Construction Tailorable Advanced Functional Materials and Green Applications, School of Materials Science and Engineering, Beijing Institute of Technology, Beijing 100081, China

 Electronic Supplementary Information

**Abstract** A series of new photodegradable poly(furan-amine)s (PFAs) were synthesized by a one-pot, catalyst-free, multicomponent cyclopolymerization between diisocyanides, dialkylacetylene dicarboxylates, and aromatic dialdehydes. All polymerizations were conducted in toluene at 100 °C for 6 h without inert gas protection and furnished polymers with a satisfactory molecular weight ( $M_w$  up to 32200) and yield. The PFA structure was confirmed by spectroscopic techniques, such as GPC, FTIR, and NMR, as well as by comparison with a model compound. The polymers exhibited good solubility in common organic solvents and thermal stability. All the PFAs had high refractive indices in the visible light region (400 nm to 800 nm). Moreover, the PFAs were substantially degraded by UV irradiation due to the presence of furan rings. The film thickness reduction rate could be over 90%.

**Keywords** Photodegradation; Multicomponent reaction; Catalyst-free polymerization

**Citation:** Fu, W. Q.; Zhu, G. N.; Shi, J. B.; Tong, B.; Cai, Z. X.; Dong, Y. P. Synthesis and properties of photodegradable poly(furan-amine)s by a catalyst-free multicomponent cyclopolymerization. *Chinese J. Polym. Sci.* 2019, 37, 981–989.

## INTRODUCTION

The degradation mechanisms of degradable polymers can generally be divided into classes such as photodegradation, mechanochemical degradation, thermal degradation, and biodegradation.<sup>[1]</sup> Among these various photoresponsive materials, photodegradable polymeric materials that can be irreversibly decomposed by irradiation have been used for cancer therapy,<sup>[2]</sup> as topographical pattern materials,<sup>[3]</sup> in photo-triggered drug delivery,<sup>[4]</sup> in dynamic 3D cell cultures,<sup>[5]</sup> and so on.<sup>[6]</sup> Photodegradable polymers can be generally divided into four types based on their degradation mechanism: main chain cleavage, side chain elimination, photodegradation of block junctions, and photolabile cross-linker cleavage.<sup>[7]</sup> The reason for the limited applications of these photodegradable polymers is that in most cases, the removal of large residual fragments requires a large amount of organic solvent, which results in environmental problems and can affect the quality of lithography products. Therefore, the development of residue-free photodegradable polymers has attracted increasing attention in recent years.<sup>[8]</sup>

Heteroaromatic polymers, such as polyfurans (PFus),<sup>[9]</sup>

polyheterocycles,<sup>[10]</sup> polythiophenes,<sup>[11]</sup> and polypyrroles,<sup>[12]</sup> have received considerable attention due to their interesting structural, electrochemical, electrical, mechanical, and optical properties. PFus modified by  $\text{FeCl}_3$ ,  $\text{SbCl}_3$ , or  $\text{HCl}$  as oxidants can show electrical conductivities several orders of magnitude higher than those of their pristine analogues.<sup>[13]</sup> However, PFus have poor thermal stability and processability.<sup>[14,15]</sup> Furthermore, PFus are difficult to obtain from furan-containing monomers because these monomers are often sensitive to light and/or acid. Therefore, new methods for the synthesis of PFus and their derivatives are of great interest. In general, improving the thermal stability of PFus and their derivatives can be realized by substituting all four sites on the furan ring.<sup>[16,17]</sup> In 2018, Tang's group developed a new, facile, alkyne-based polymerization using oxygen to obtain functional poly(tetrasubstituted furan)s with high thermal stability.<sup>[18]</sup>

Multicomponent cyclopolymerizations (MCCs) are one-pot reactions of three or more monomers to directly afford polymers containing a new ring, such as a thiophene<sup>[19]</sup> or pyrimidine.<sup>[20]</sup> Developing new MCCs is very important because they offer many advantages, such as structural controllability, molecular weight controllability, wide applicability, and high atom economy.<sup>[21]</sup> In 2016, Arndtsen's group developed a new MCC to prepare a pyrrole-based  $\pi$ -conjugated polymer by the reaction of alkynes, imines, and acid chlorides using a metal-free catalyst.<sup>[22]</sup> Currently, alkynes and isocyanides are among the monomers commonly used

\* Corresponding authors: E-mail [bing@bit.edu.cn](mailto:bing@bit.edu.cn) (J.B.S.)  
E-mail [chdongyp@bit.edu.cn](mailto:chdongyp@bit.edu.cn) (Y.P.D.)

Invited article for special issue of "The 100<sup>th</sup> Anniversary of the Birth of Prof. Shi-Lin Yang"

Received March 20, 2019; Accepted April 22, 2019; Published online June 20, 2019

for developing these new polymerization reactions.<sup>[23–26]</sup> Recently, we also developed an efficient, one-pot, catalyst-free MCC of a diisocyanide, a dialkylacetylene dicarboxylate (DAAD), and a dialdehyde.<sup>[27]</sup> By changing the polymerization conditions, a series of poly(amine-furan-arylene)s were obtained with high structural controllability, and all of the polymers showed good thermal stability and thin-film processability.

Based on our previous work, we extended this system to additional aromatic dialdehyde monomers, including those with other heterocyclic spacers such as pyrimidine, quinoxaline, pyridine, and thiophene. We prepared a series of poly(furan-amine)s (PFAs) by reacting diisocyanide and DAAD first and then with different aromatic heterocyclic dialdehydes under catalyst-free polymerization conditions, and the method offers high atom economy and operational simplicity. All the obtained PFAs showed good solubility in common organic solvents such as dichloromethane (DCM), tetrahydrofuran (THF), chloroform, dimethylsulfoxide (DMSO), and *N,N*-dimethyl formamide (DMF). The structures of the obtained PFAs were confirmed by GPC, FTIR, and NMR spectroscopy and compared with that of the model compound (MC). All the PFAs possessed high refractive indices in the visible light region. Moreover, the photostabilities of these PFAs were studied, which indicated their potentials of degrading into volatile products with low molecular weights and/or small amounts of residual fragments under ultraviolet light. Thus, this MCC resulted in useful photodegradable materials, which may offer a new platform for the design of multifunctional PFUs.

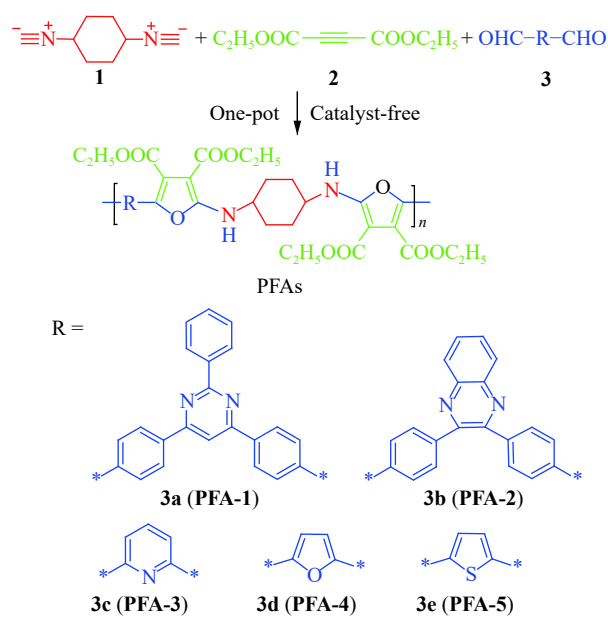
## EXPERIMENTAL

### Materials

Diisocyanide **1** and dialdehyde **3a** were prepared according to our previous work.<sup>[27]</sup> Dialdehyde monomer **3b**, as shown in Scheme 1, was prepared by the reported procedure with some modifications, and the structural characterization data are shown in the electronic supplementary information (ESI).<sup>[28]</sup> Dialdehydes **3c**, **3d**, and **3e**, DAAD, and cyclohexyl isocyanide **4** are commercial products purchased from Energy Chemical. If not specifically indicated, all reagents were used as received without further purification.

### Measurements

The weight-average molecular weight ( $M_w$ ) and polydispersity index ( $M_w/M_n$ ) of each PFA were obtained from gel permeation chromatography (GPC) using a Waters 1515 isocratic HPLC pump and a Waters 2414 refractive index detector. Polystyrene was used as the standard, and THF was used as the eluent at a flow rate of 1.0 mL/min. Mass spectra were collected by using a Finnigan BIFLEX III mass spectrometer. The X-ray crystal structure data were collected on a Bruker-AXS SMART APEX2 CCD diffractometer. Fourier transform infrared (FTIR) spectra were recorded on a Bruker (ALPHA) spectrometer. NMR spectra were measured on a Bruker AV 400 spectrometer. Thermogravimetric analysis (TGA) was carried out on a PerkinElmer STA 8000 at a heating rate of 10 °C/min under flowing nitrogen. UV-Vis



Scheme 1 Synthetic route to polymers

spectra were recorded on a TU-1901 double beam UV-Vis spectrophotometer. Fluorescence spectra were obtained from a Hitachi F-7000 fluorescence spectrophotometer. The refractive indices were measured on a SENTECH SE 850 DUV spectroscopic ellipsometer. Ultraviolet light experiments were carried out with a 365 nm wavelength UV lamp with 9000  $\mu\text{W}/\text{cm}^2$  of power.

### Synthetic Procedure of MC

To a 30-mL Schlenk tube equipped with a magnetic stir bar were added cyclohexyl isocyanide (**4**, 0.1090 g, 1.0 mmol), **2** (0.1700 g, 1.0 mmol), **3a** (0.1460 g, 0.4 mmol), and 3 mL of toluene. The reaction mixture was heated in a heating jacket at 100 °C for 6 h under constant stirring under an air atmosphere and then cooled to room temperature. The organic layer was washed by water, extracted with DCM, combined together, and then dried over  $\text{MgSO}_4$  for 1 h. **MC** was purified by flash column chromatography.

### Synthetic Procedure of PFA-1

The MCC procedure is described using **PFA-1** as an example. To a 30-mL Schlenk tube equipped with a magnetic stir bar, monomer **1** (67.0 mg, 0.5 mmol), monomer **2** (170.0 mg, 1.0 mmol), monomer **3a** (145.6 mg, 0.4 mmol), and toluene (6 mL) were added. The reaction mixture was heated in a heating jacket at 100 °C for 6 h under an air atmosphere. After being cooled to room temperature and dropped into 150 mL of *n*-hexane under vigorous stirring, the precipitate was isolated by filtration, washed with *n*-hexane, and dried to a constant weight in a vacuum drying oven at 60 °C to afford **PFA-1**. The MCCs of **PFA-2–PFA-5** followed the same procedure with the appropriate dialdehyde monomer (**3b–3e**).

### Characterization Data of MC and PFA-1–PFA-5

#### Characterization data for MC

Yellow solid; IR ( $\nu$ ,  $\text{cm}^{-1}$ ): 3355, 2979, 1729, 1672, 1619, 1466, 1216, 1105, 1038;  $^1\text{H-NMR}$  (400 MHz,  $\text{CDCl}_3$ ,  $\delta$ ,

ppm): 8.73–8.71 (m, 2H), 8.73–8.71 (d,  $J = 8.4$  Hz, 2H), 7.99 (s, 1H), 7.71–7.69 (d,  $J = 8.8$  Hz, 4H), 7.55–7.53 (m, 3H), 6.70–6.68 (d,  $J = 8.0$  Hz, 2H), 4.46–4.41 (m, 4H), 4.28–4.23 (m, 4H), 3.75 (s, 2H), 2.09–2.07 (m, 4H), 1.83–1.80 (m, 4H), 1.68–1.65 (m, 2H), 1.44–1.40 (m, 14H), 1.34–1.30 (m, 8H);  $^{13}\text{C-NMR}$  (100 MHz,  $\text{CDCl}_3$ ,  $\delta$ , ppm): 165.46, 164.49, 164.41, 163.86, 161.42, 139.56, 137.97, 135.80, 131.60, 130.76, 128.54, 128.46, 127.62, 124.44, 115.47, 109.63, 88.26, 61.86, 59.77, 51.59, 33.48, 25.47, 24.58, 14.45, 14.17. HRMS (ESI,  $m/z$ ) Calcd. for  $[\text{M}+\text{Na}]^+$   $\text{C}_{54}\text{H}_{58}\text{N}_4\text{O}_{10}\text{Na}$ : 945.4051, Found: 945.4045, Error: 0.6 ppm.

#### Characterization data for **PFA-1**

Yellow solid;  $M_w$ : 31900;  $M_n$ : 9800; DP: 12; IR ( $\nu$ ,  $\text{cm}^{-1}$ ): 3349, 2980, 1729, 1674, 1611, 1468, 1215, 1097, 1034;  $^1\text{H-NMR}$  (400 MHz,  $\text{CDCl}_3$ ,  $\delta$ , ppm): 8.72–7.51 (aromatic protons), 6.70 (amino protons), 4.45–4.26 ( $\text{OCH}_2$  protons), 3.83 (CH protons), 2.29–1.24;  $^{13}\text{C-NMR}$  (100 MHz,  $\text{CDCl}_3$ ,  $\delta$ , ppm): 165.31, 164.49, 163.67, 161.18, 139.96, 138.06, 136.12, 131.37, 130.71, 128.45, 127.60, 124.50, 115.32, 109.54, 88.77, 61.92, 59.92, 51.00, 31.94, 29.70, 21.05, 14.43, 14.16.

#### Characterization data for **PFA-2**

Yellow solid;  $M_w$ : 6600;  $M_n$ : 3600; DP: 5; IR ( $\nu$ ,  $\text{cm}^{-1}$ ): 3347, 2980, 1729, 1674, 1611, 1468, 1217, 1097, 1034;  $^1\text{H-NMR}$  (400 MHz,  $\text{CDCl}_3$ ,  $\delta$ , ppm): 8.17–7.54 (aromatic protons), 6.64 (amino protons), 4.38–4.25 ( $\text{OCH}_2$  protons), 3.79 (CH protons), 2.25–1.31;  $^{13}\text{C-NMR}$  (100 MHz,  $\text{CDCl}_3$ ,  $\delta$ , ppm): 165.25, 164.37, 161.06, 152.47, 151.85, 144.98, 141.50, 141.21, 139.88, 136.19, 130.57, 130.27, 129.71, 129.28, 129.17, 124.10, 114.96, 88.56, 61.82, 59.82, 50.76, 31.94, 14.41, 14.07.

#### Characterization data for **PFA-3**

Gray solid;  $M_w$ : 7900;  $M_n$ : 4000; DP: 7; IR ( $\nu$ ,  $\text{cm}^{-1}$ ): 3351, 2986, 1676, 1562, 1238, 1171, 1079, 977;  $^1\text{H-NMR}$  (400 MHz,  $\text{CDCl}_3$ ,  $\delta$ , ppm): 7.78–7.33 (aromatic protons), 6.56 (amino protons), 4.38–4.17 ( $\text{OCH}_2$  protons), 3.73 (CH protons), 2.25–1.22;  $^{13}\text{C-NMR}$  (100 MHz,  $\text{CDCl}_3$ ,  $\delta$ , ppm): 164.84, 164.66, 161.39, 152.41, 148.48, 147.69, 137.71, 136.84, 121.11, 118.84, 118.47, 117.62, 116.58, 89.16, 61.73, 60.04, 50.80, 32.33, 31.85, 14.37, 14.22, 14.11.

#### Characterization data for **PFA-4**

Yellow solid;  $M_w$ : 14800;  $M_n$ : 6700; DP: 11; IR ( $\nu$ ,  $\text{cm}^{-1}$ ): 3345, 2980, 1729, 1672, 1605, 1462, 1224, 1097, 1066;  $^1\text{H-NMR}$  (400 MHz,  $\text{CDCl}_3$ ,  $\delta$ , ppm): 6.66 (furan, amino protons), 4.37–4.25 ( $\text{OCH}_2$  protons), 3.76 (CH protons), 2.23–1.31;  $^{13}\text{C-NMR}$  (100 MHz,  $\text{CDCl}_3$ ,  $\delta$ , ppm): 164.58, 163.73, 161.18, 143.73, 134.17, 113.81, 109.24, 100.00, 87.67, 61.50, 59.86, 50.74, 32.02, 14.42, 14.20.

#### Characterization data for **PFA-5**

Yellow solid;  $M_w$ : 17200;  $M_n$ : 6100; DP: 10; IR ( $\nu$ ,  $\text{cm}^{-1}$ ): 3343, 2980, 1729, 1666, 1610, 1456, 1213, 1097;  $^1\text{H-NMR}$  (400 MHz,  $\text{CDCl}_3$ ,  $\delta$ , ppm): 7.25 (thiophene protons), 6.67 (amino protons), 4.39–4.24 ( $\text{OCH}_2$  protons), 3.75 (CH protons), 2.24–1.30;  $^{13}\text{C-NMR}$  (100 MHz,  $\text{CDCl}_3$ ,  $\delta$ , ppm): 164.56, 164.19, 160.94, 138.06, 130.41, 124.91, 113.40, 88.05, 61.58, 59.86, 50.77, 31.83, 14.39, 14.18.

## RESULTS AND DISCUSSION

### Polymerization and Structural Characterization

With the optimized polymerization conditions developed in our previous work,<sup>[27]</sup> various combinations of dialdehydes **3a–3e** were investigated, and the results are shown in Table 1. The MCCs proceeded smoothly and afforded the target PFAs with good solubilities and in high yields (up to 86.6%). **PFA-1** was obtained in the highest yield and had the highest  $M_w$ , mainly attributable to its twisted three-dimensional structure and less steric hindrance, which favored the polymerization. However, it is worth noting that **PFA-2** exhibited low  $M_w$  values probably due to the more coplanar, conjugated structure of monomer **3b**, which resulted in more  $\pi$ - $\pi$  stacking of rigid main chains, blocking further chain growth and thereby producing low-molecular-weight products.<sup>[29,30]</sup> 2,6-Substituted pyridinyl of monomer **3c** actually deactivated the aldehyde group, which resulted in low yield and molecular weight of **PFA-3**. 2,5-Substituted monomers **3d** and **3e** were tested, and the resulting polymers, **PFA-4** and **PFA-5**, had higher  $M_w$  values, which was mainly due to the higher activity of aldehyde group when linked with thiophene and furan groups. All these results indicated that the activity of the aldehyde group as well as coplanarity and conjugated degree of monomers should be considered in this MCC. To confirm the PFA structures, a model compound, **MC**, was efficiently prepared by reacting monomers **2** and **3a** with cyclohexyl isocyanide (**4**, a mono-isocyanide) under the same experimental conditions, as shown in Scheme 2, to facilitate the comparison of certain key signals. Fortunately, we obtained a single crystal of **MC** by slow evaporation from a DCM/hexane solution, and its monomolecular configuration is shown in Fig. 1. The target cyclization indeed occurred in the abovementioned experiments, and the desired furan rings were formed. Moreover, there were intramolecular hydrogen bonds between O of the carboxyl groups and H of the amine groups, which would extend the tunability of photophysical properties and thermal stabilities of these compounds.

**Table 1** MCC data from the polymerizations of monomers **1**, **2**, and **3**<sup>a</sup>

Entry	PFAs	Monomers	Yield (%)	$M_w^b \times 10^{-4}$	$D^b$	Solubility <sup>c</sup>
1	<b>PFA-1</b>	<b>1 + 2 + 3a</b>	86.6	3.19	3.26	○
2	<b>PFA-2</b>	<b>1 + 2 + 3b</b>	79.6	0.66	1.83	○
3	<b>PFA-3</b>	<b>1 + 2 + 3c</b>	77.4	0.79	1.98	○
4	<b>PFA-4</b>	<b>1 + 2 + 3d</b>	80.5	1.48	2.21	○
5	<b>PFA-5</b>	<b>1 + 2 + 3e</b>	75.8	1.72	2.82	○

<sup>a</sup> Carried out in toluene under air at 100 °C for 6 h,  $[\mathbf{1}] = 0.08$  mol/L,  $\mathbf{1}:\mathbf{2}:\mathbf{3} = 1:2:0.8$ ; <sup>b</sup> Determined by GPC in THF using linear polystyrenes as the calibration standards.  $M_w$  is the weight-average molecular weight;  $D = M_w/M_n$ , where  $M_n$  is the number-average molecular weight; <sup>c</sup> ○: completely soluble in THF, DMSO, and DMF

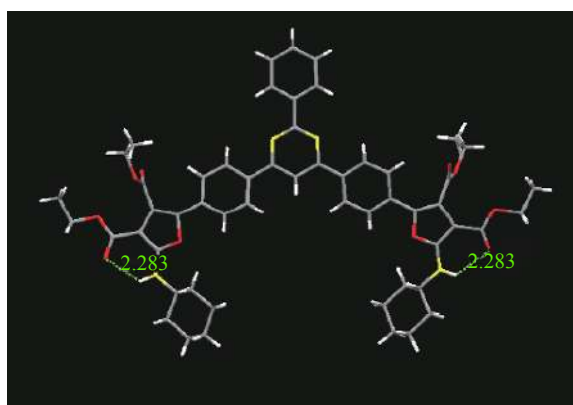
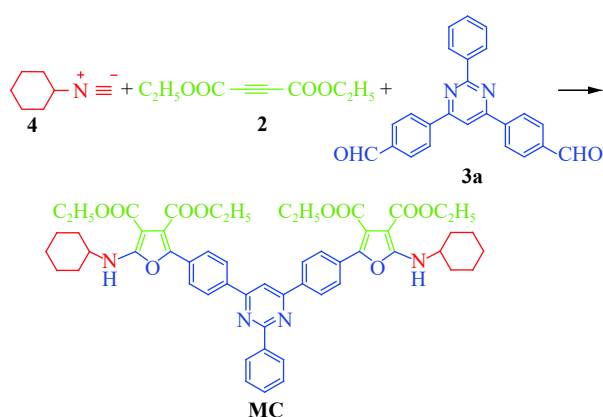


**Fig. 1** Crystal structure of MC (CCDC-1891535). C atoms are shown in gray, H atoms are shown in white, O atoms are shown in red, and N atoms are shown in yellow.

All PFAs were characterized by spectroscopic techniques, such as NMR and FTIR spectroscopy. Since all PFAs have similar structures, we take **PFA-1** as an example to investigate the key features of MCC. First, the FTIR spectra of **1**, **2**, **3a**, **MC**, and **PFA-1**, shown in Fig. 2, confirmed the polymer structure, since the structure of **MC** was clearly confirmed by its single crystal. The stretching vibration of  $\text{N}\equiv\text{C}$  is located at  $2135\text{ cm}^{-1}$  in monomer **1** (Fig. 2a), and the analogous band is not present in the spectra of either **MC** or **PFA-1** (Figs. 2d and 2e). The stretching vibration of  $\text{C}=\text{O}$ , located at  $1723\text{ cm}^{-1}$  in monomer **2** (Fig. 2b), appears at different wavenumbers ( $1729$  and  $1674\text{ cm}^{-1}$ ) in the spectra of **MC** and **PFA-1** after the formation of furan rings mainly because the chemical environments of the carbonyl groups in **MC** and **PFA-1** are different.<sup>[31]</sup> Additionally, the  $\text{C}=\text{C}$  and  $\text{N}-\text{H}$  stretching vibrations appear at  $1611$  and  $3349\text{ cm}^{-1}$  in the spectra of **MC** and **PFA-1**, respectively, and these bands could be attributed to the furan and amino groups. The new band at  $1097\text{ cm}^{-1}$  in the spectra of **MC** and **PFA-1** is due to the stretching vibration of  $\text{C}-\text{O}$  in the furan rings. All these changes indicate that MCCs conducted under the optimized experimental conditions produced the target polymers. The FTIR spectra of other polymers showed similar results, and these spectra are presented in Figs. S1–S4 (in ESI).

The  $^1\text{H}$ - and  $^{13}\text{C}$ -NMR spectra of **1**, **2**, **3a**, **MC**, and **PFA-1** are given in Figs. 3 and 4. The characteristic  $\text{H}_a$  resonance of **1** at  $\delta = 3.80\text{ ppm}$  is observed at  $3.78$  and  $3.81\text{ ppm}$  in the  $^1\text{H}$ -NMR spectra of **MC** and **PFA-1**, respectively. The  $\text{H}_b$  resonance of **2** at  $\delta = 4.28\text{ ppm}$  splits into two signals,  $\text{H}_{b1}$  and  $\text{H}_{b2}$  for **MC** and  $\text{H}_{b1'}$  and  $\text{H}_{b2'}$  for **PFA-1**, and this is attributed to the two kinds of newly formed  $\text{CH}_2$  protons on

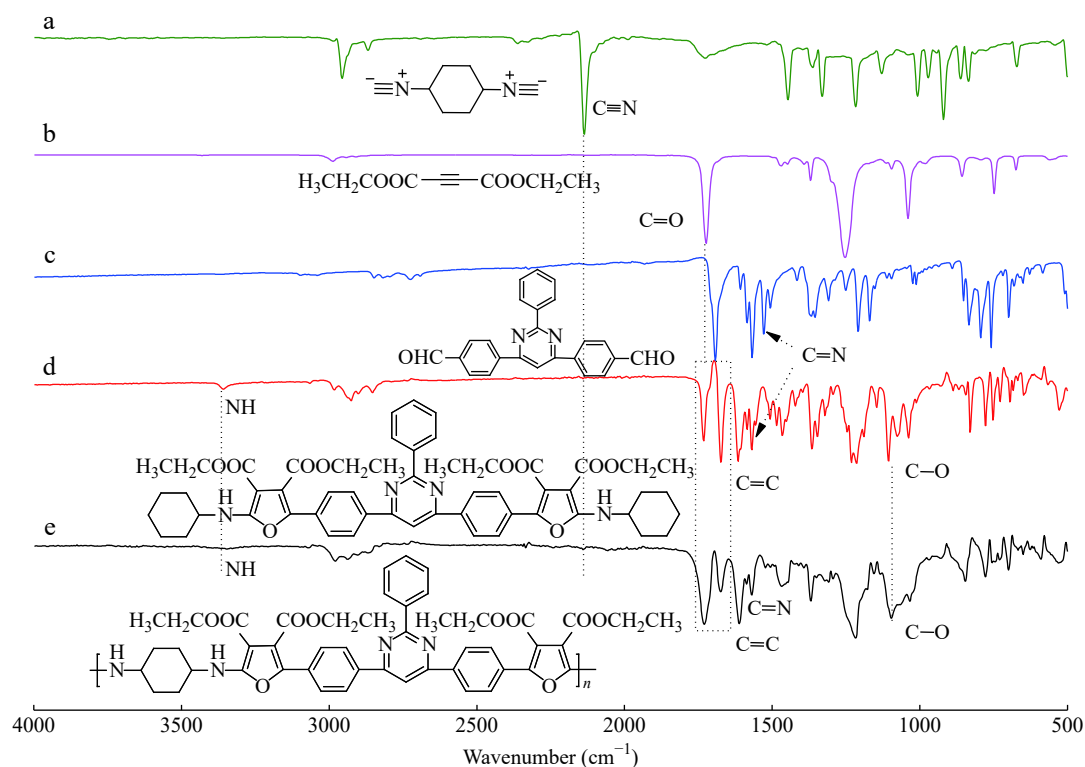


**Fig. 2** FTIR spectra of (a) **1**, (b) **2**, (c) **3a**, (d) **MC**, and (e) **PFA-1**

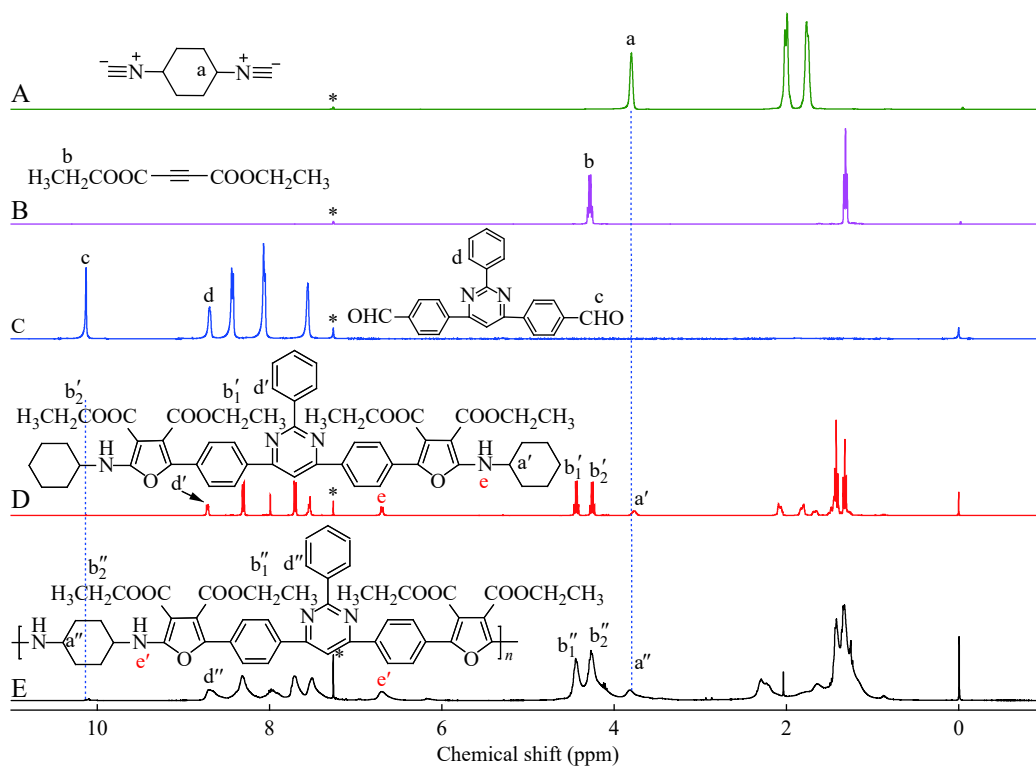


**Fig. 3**  $^1\text{H}$ -NMR spectra of (A) **1**, (B) **2**, (C) **3a**, (D) **MC**, and (E) **PFA-1** in  $\text{CDCl}_3$ . The solvent peaks are marked with asterisks.

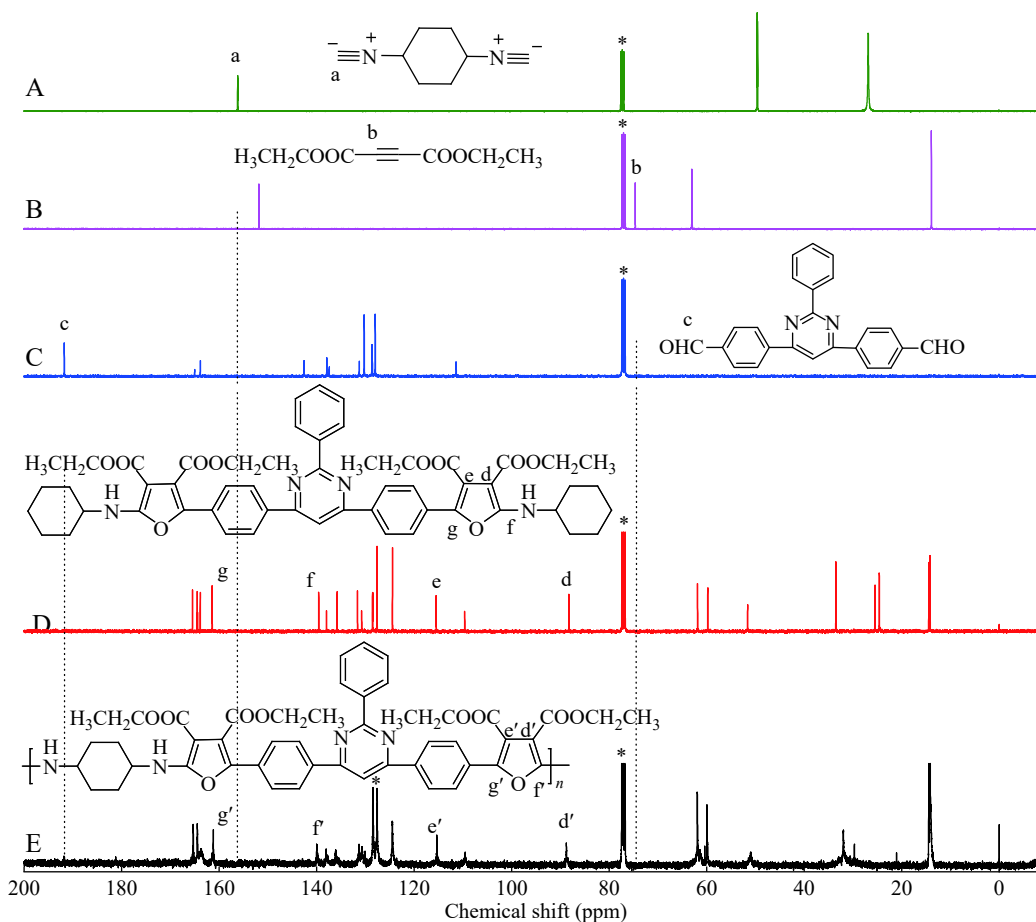


**Fig. 4**  $^{13}\text{C}$ -NMR spectra of (A) **1**, (B) **2**, (C) **3a**, (D) **MC**, and (E) **PFA-1** in  $\text{CDCl}_3$ . The solvent peaks are marked with asterisks.

the furan rings. A new signal at  $\delta = 6.70$  ppm assigned to the amino proton of  $H_c$  in **MC** appears at the same chemical shift as  $H_c$  in the spectrum of **PFA-1**. The results from  $^1H$ -NMR analyses indicated that MCCs proceeded smoothly *via* this simple one-pot procedure. Furthermore, the resonance signals of  $C_a$  in **1** at  $\delta = 156.91$  ppm and  $C_b$  in **2** at  $\delta = 77.36$  ppm are absent in the  $^{13}C$ -NMR spectra of **MC** and **PFA-1**. The four new signals located at  $\delta = 88.26$ , 115.47, 139.56, and 161.42 ppm are assigned to the resonances of  $C_d$ ,  $C_e$ ,  $C_f$ , and  $C_g$  in **MC**, and the signals at 88.75, 115.32, 139.98, and 161.18 ppm are attributed to the resonances of  $C_d$ ,  $C_e$ ,  $C_f$ , and  $C_g$  in **PFA-1**, which confirmed that the furan rings were formed during MCC.[32] Other features of the  $^1H$ - and  $^{13}C$ -NMR spectra of these PFAs were similar, and they are presented in Figs. S5–S12 (in ESI).

### Thermal Stability

As shown in Fig. 5, the thermal stabilities of these PFAs were evaluated by thermogravimetric analysis (TGA). The initial decomposition temperatures of all the samples (corresponding to 5% weight loss,  $T_d$ ) ranged from 260 °C to 268 °C under a  $N_2$  atmosphere, which indicated that all the PFAs were thermally stable.[33] The improved stability of the PFAs is probably due to the intermolecular or intramolecular hydrogen bonds between the O atoms on carboxyl groups and the H atoms on amine groups, as shown in the above-mentioned single crystal of **MC**. The higher  $T_d$  values of **PFA-2** and **PFA-3** were probably due to the increased  $\pi$ - $\pi$  interactions between main chains,[18] which is consistent with the lower  $M_w$  values.

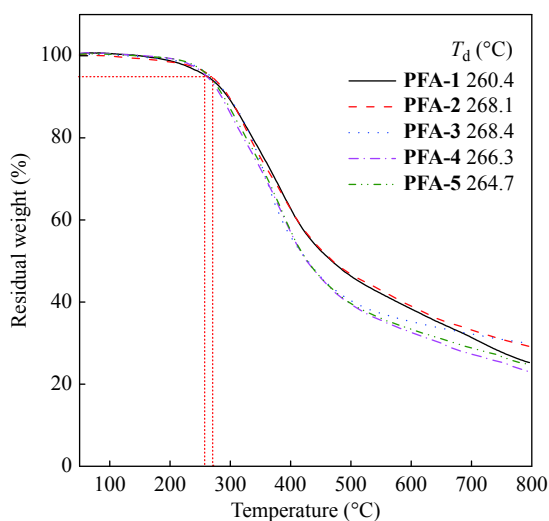


Fig. 5 Thermograms of **PFA-1**, **PFA-2**, **PFA-3**, **PFA-4**, and **PFA-5** measured under  $N_2$  at a heating rate of 10 °C/min

### Light Refractivity

Polymeric materials with a high refractive index (RI) attract significant interest because of the greater impact resistance, better processability, lightweight, and higher dyeing ability compared to the inorganic glasses, which has been widely used as organic light-emitting diodes (OLEDs), antireflective coatings, arrays of prisms, charge-coupled devices (CCDs) for digital cameras, etc.[34] Heteroatom-containing polymers usually show high refractive indices (RI values).[35]

Therefore, these PFAs, which contain nitrogen and oxygen atoms in every repeat unit, were predicted to have high RI values. Films of the obtained PFAs were then prepared by a spin-coating process, and their RI values were measured in the spectral region of 400–800 nm, as shown in Fig. 6. All the PFAs showed high RI values, especially **PFA-1**, which had the highest RI, probably due to its highest  $M_w$ . All these PFAs exhibited higher RI values than those of commercially important optical polymeric materials, such as polystyrene ( $n = 1.587$  at 632.8 nm) and polycarbonate ( $n = 1.581$  at 632.8 nm).

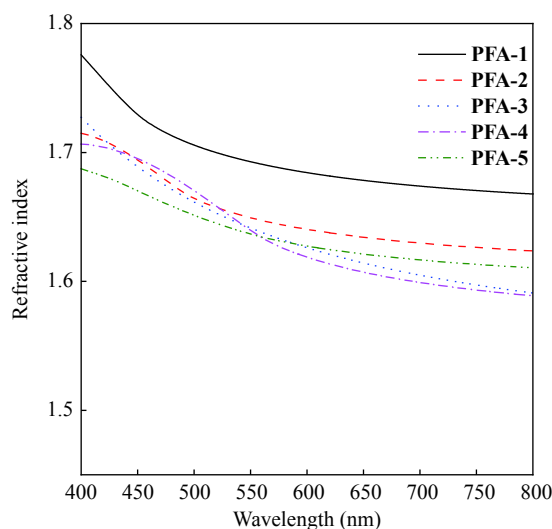
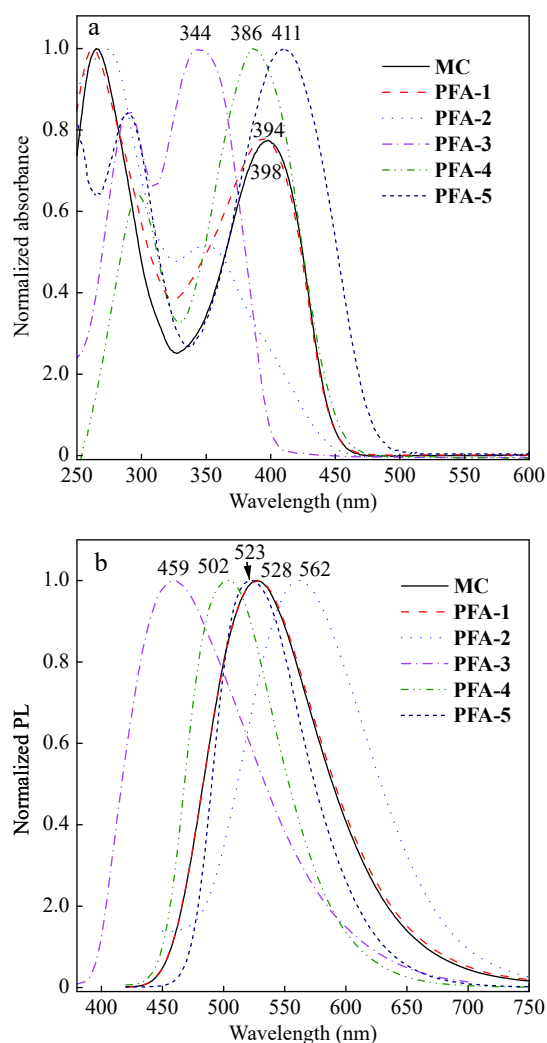


Fig. 6 Refractive indices of thin films of **PFA-1**, **PFA-2**, **PFA-3**, **PFA-4**, and **PFA-5**

### Photophysical Properties

The normalized UV-Vis absorption spectra of **MC** and PFAs were obtained from their THF solutions (Fig. 7a). The UV absorption peaks of **MC** and **PFA-1** are similar and centered at approximately 263 and 395 nm; the peaks at a shorter wavelength are attributed to the  $\pi$ - $\pi^*$  transition of benzene rings, and the ones at longer wavelength result from the  $\pi$ - $\pi^*$  transition of conjugated backbone. The absorption maximum of **PFA-5** appears at the longest wavelength (411 nm), which is probably due to the presence of thiophene rings that have strong electron donating abilities and thus exert a D-A effect on the ester groups.[36] The photoluminescence (PL) spectra of PFAs in THF are shown in Fig. 7(b). **MC**, **PFA-1**, **PFA-2**, **PFA-3**, **PFA-4**, and **PFA-5** exhibited one emission peak centered at 528, 528, 562, 459, 502, and 523 nm, respectively. **PFA-2** had a longer emission wavelength than other PFAs due to the presence of quinoxaline groups, which are relatively planar. The PL properties of **MC** and **PFA-1** were investigated in THF and in  $H_2O$  (Figs. S13 and S14 in ESI), and their PL intensities gradually decreased with increasing water content, which was consistent with the typical aggregation-induced quenching.[37,38]

Polymers containing furan rings are often used as photo-degradable materials because furan rings are sensitive to light.[39] As shown in Fig. 8(a), UV-Vis absorption spectra of **PFA-1** were collected after predetermined durations of irradiation under a 365 nm UV lamp. The results indicated that



**Fig. 7** Normalized (a) UV-Vis absorption and (b) PL spectra of MC, PFA-1, PFA-2, PFA-3, PFA-4, and PFA-5 in THF (10  $\mu\text{mol/L}$ )

the UV absorption band from the  $\pi\text{-}\pi^*$  transition of the conjugated backbone disappeared after 20 min of irradiation, which suggests that the PFAs were photodegradable. At the same time, the fluorescence of PFA-1 was also substantially lower after 20 min of irradiation, as shown in Fig. 8(b). All these results indicate that this PFA was highly sensitive to UV light and could potentially be used for lithography applications. Ellipsometry tests showed that the film thickness reduction rate of PFA-1 was up to 90% after 120 min of UV irradiation (Table 2). The sensitivity of the furan rings to light might cause main chain degradation in these polymers.<sup>[40,41]</sup> The UV traces of the other PFAs showed similar trends (Figs. S15–S18 in ESI). In addition, NMR spectra of MC indicated the breakage of C–NH and ring opening of furan, as shown in Figs. S19 and S20 (in ESI). GPC tracking of PFA-1 in THF at different irradiation time also verified the occurrence of photodegradation into small segments (Fig. S21 in ESI). Therefore, this MCC is a very useful method for preparing photodegradable polymers with a small amount of residual fragment. Experiments to fully elucidate the photodegradation mechanism are under way in our laboratory and will be reported in due course.

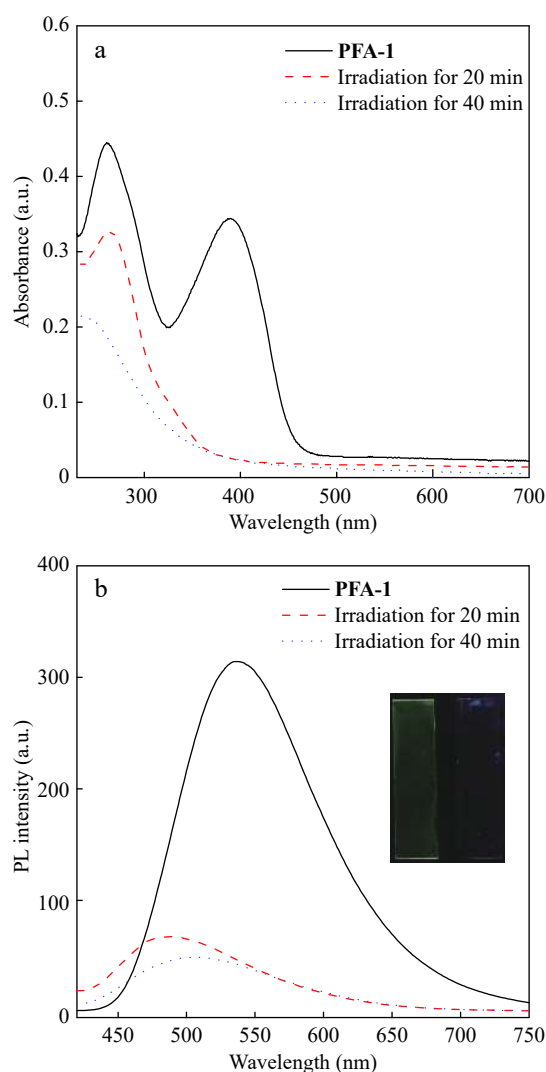


**Fig. 8** (a) UV-Vis absorption and (b) PL spectra of thin solid films of PFA-1 after different irradiation time (Inset: photos of the solid films of PFA-1 before (left) and after (right) 20 min of irradiation)

**Table 2** The reduction rate of the solid film thickness<sup>a</sup>

Entry	PFAs	Reduction rate <sup>b</sup> (%)		
		20 min	40 min	120 min
1	PFA-1	48.5	58.9	91.6
2	PFA-2	11.3	18.7	30.6
3	PFA-3	33.3	52.3	68.6
4	PFA-4	21.5	31.4	52.9
5	PFA-5	13.7	16.9	79.5

<sup>a</sup> The PFAs were irradiated under a 9000  $\mu\text{W}/\text{cm}^2$ , 365 nm UV lamp; <sup>b</sup> The values of the reduction rate were calculated from the film thickness before and after irradiation, and the film thicknesses were measured by an ellipsometer

## CONCLUSIONS

In summary, five PFAs were synthesized *via* a one-pot, catalyst-free MCC of a diisocyanide, DAAD, and an aromatic dialdehyde. This MCC could proceed without inert gas protection. Their key structural features were verified by GPC, FTIR, and NMR techniques. PFAs with good solubility possessed good film processability and exhibited high thermal stability and refractive index values. These PFAs could be

degraded under UV light due to the presence of furan rings, which makes them potentially applicable as photoetching materials. Thus, this MCC may serve as a new method for preparing photodegradable polymers.

### Electronic Supplementary Information

Electronic supplementary information (ESI) is available free of charge in the online version of this article at <http://dx.doi.org/10.1007/s10118-019-2281-5>.

### ACKNOWLEDGMENTS

This work was financially supported by the National Natural Science Foundation of China (Nos. 21490574, 21875019, 51673024, and 51803009) and Beijing Institute of Technology Research Fund Program for Young Scholars.

### REFERENCES

- Nayanathara, U.; Kottegoda, N.; Perera, I. C.; Mudiyansele, T. K. Synthesis, photodegradable and antibacterial properties of polystyrene-cinnamaldehyde copolymer film. *Polym. Degrad. Stab.* **2018**, *155*, 195–207.
- Pan, G. Y.; Jia, H. R.; Zhu, Y. X.; Wu, F. G. Turning double hydrophilic into amphiphilic: IR825-conjugated polymeric nanomicelles for near-infrared fluorescence imaging-guided photothermal cancer therapy. *Nanoscale* **2018**, *10*, 2115–2127.
- Fairbanks, B. D.; Singh, S. P.; Bowman, C. N.; Anseth, K. S. Photodegradable, photoadaptable hydrogels via radical-mediated disulfide fragmentation reaction. *Macromolecules* **2011**, *44*, 2444–2450.
- Cao, Z.; Li, Q.; Wang, G. Photodegradable polymer nanocapsules fabricated from dimethyldiethoxysilane emulsion templates for controlled release. *Polym. Chem.* **2017**, *8*, 6817–6823.
- Käpylä, E.; Delgado, S. M.; Kasko, A. M. Shape-changing photodegradable hydrogels for dynamic 3D cell culture. *ACS Appl. Mater. Interfaces* **2016**, *8*, 17885–17893.
- McKinnon, D. D.; Brown, T. E.; Kyburz, K. A.; Kiyotake, E.; Anseth, K. S. Design and characterization of a synthetically accessible, photodegradable hydrogel for user-directed formation of neural networks. *Biomacromolecules* **2014**, *15*, 2808–2816.
- Manouras, T.; Vamvakaki, M. Field responsive materials: Photo-, electro-, magnetic- and ultrasound-sensitive polymers. *Polym. Chem.* **2017**, *8*, 74–96.
- Yang, F. C.; Wang, J.; Chen, L.; Wang, X.; Chen, X. Y.; Zhang, X. Soluble and degradable polyimides with phenyl-2-pyridyl ether structure: Synthesis and characterization. *Chinese J. Polym. Sci.* **2015**, *33*, 481–489.
- Liu, Y.; Yuan, J.; Zou, Y.; Li, Y. Research progress of the furan-containing fused ring conjugated organic molecules and polymers. *Acta Chim. Sin.* **2017**, *75*, 257–270.
- Hu, Y.; Han, T.; Yan, N.; Liu, J.; Liu, X.; Wang, W. X.; Lam, J. W. Y.; Tang, B. Z. Visualization of biogenic amines and *in vivo* ratiometric mapping of intestinal pH by AIE-active polyheterocycles synthesized by metal-free multicomponent polymerizations. *Adv. Funct. Mater.* **2019**, 1902240.
- Wang, F.; Gu, H.; Swager, T. M. Carbon nanotube/polythiophene chemiresistive sensors for chemical warfare agents. *J. Am. Chem. Soc.* **2008**, *130*, 5392–5393.
- Afzal, A.; Abulailwi, F. A.; Habib, A.; Awais, M.; Waje, S. B.; Atieh, M. A. Polypyrrole/carbon nanotube supercapacitors: Technological advances and challenges. *J. Power Sources* **2017**, *352*, 174–186.
- Tibaoui, T.; Zaidi, B.; Bouachrine, M.; Paris, M.; Alimi, K. A study of polymers obtained by oxidative coupling of furan monomers. *Synth. Met.* **2011**, *161*, 2220–2225.
- Yeh, I. C.; Rinderspacher, B. C.; Andzelm, J. W.; Cureton, L. T.; La Scala, J. Computational study of thermal and mechanical properties of nylons and bio-based furan polyamides. *Polymer* **2014**, *55*, 166–174.
- Streifel, B. C.; Martínez Hardigree, J. F.; Katz, H. E.; Tovar, J. D. Heteroaromatic variation in amorphous 1,6-methano[10]annulene-based charge-transporting organic semiconductors. *J. Mater. Chem. C* **2014**, *2*, 7851–7858.
- Sousa, A. F.; Vilela, C.; Fonseca, A. C.; Matos, M.; Freire, C. S. R.; Gruter, G. J. M.; Coelho, J. F. J.; Silvestre, A. J. D. Biobased polyesters and other polymers from 2,5-furandicarboxylic acid: A tribute to furan excellency. *Polym. Chem.* **2015**, *6*, 5961–5983.
- Kaur, S.; Findlay, N. J.; Coomer, F. C.; Berridge, R.; Skabara, P. J. Poly([1,4]dithiino[2,3-*c*]furan): The synthesis, electrochemistry, and optoelectronic properties of a furan-containing polymer. *Macromol. Rapid Commun.* **2013**, *34*, 1330–1334.
- Song, B.; Hu, K.; Qin, A.; Tang, B. Z. Oxygen as a crucial comonomer in alkyne-based polymerization toward functional poly(tetrasubstituted furan)s. *Macromolecules* **2018**, *51*, 7013–7018.
- Deng, H.; Hu, R.; Zhao, E.; Chan, C. Y. K.; Lam, J. W. Y.; Tang, B. Z. One-pot three-component tandem polymerization toward functional poly(arylene thiophenylene) with aggregation-enhanced emission characteristics. *Macromolecules* **2014**, *47*, 4920–4929.
- Huang, Y.; Chen, P.; Wei, B.; Hu, R.; Tang, B. Z. Aggregation-induced emission-active hyperbranched poly(tetrahydropyrimidine)s synthesized from multicomponent tandem polymerization. *Chinese J. Polym. Sci.* **2019**, *37*, 428–436.
- Hu, R.; Li, W.; Tang, B. Z. Recent advances in alkyne-based multicomponent polymerizations. *Macromol. Chem. Phys.* **2016**, *217*, 213–224.
- Kayser, L. V.; Vollmer, M.; Welnhöfer, M.; Krickciokat, H.; Meerholz, K.; Arndtsen, B. A. Metal-free, multicomponent synthesis of pyrrole-based  $\pi$ -conjugated polymers from imines, acid chlorides, and alkynes. *J. Am. Chem. Soc.* **2016**, *138*, 10516–10521.
- Fu, W.; Dong, L.; Shi, J.; Tong, B.; Cai, Z.; Zhi, J.; Dong, Y. Synthesis of polyquinolines via one-pot polymerization of alkyne, aldehyde, and aniline under metal-free catalysis and their properties. *Macromolecules* **2018**, *51*, 3254–3263.
- Liu, Y.; Qin, A.; Tang, B. Z. Polymerizations based on triple-bond building blocks. *Prog. Polym. Sci.* **2018**, *78*, 92–138.
- Fu, W.; Dong, L.; Shi, J.; Tong, B.; Cai, Z.; Zhi, J.; Dong, Y. Multicomponent spiropolymerization of diisocyanides, alkynes and carbon dioxide for constructing 1,6-dioxospiro[4,4]nonane-3,8-diene as structural units under one-pot catalyst-free conditions. *Polym. Chem.* **2018**, *9*, 5543–5550.
- Deng, X. X.; Li, L.; Li, Z. L.; Lv, A.; Du, F. S.; Li, Z. C. Sequence regulated poly(ester-amide)s based on passerini reaction. *ACS Macro Lett.* **2012**, *1*, 1300–1303.
- Fu, W.; Kong, L.; Shi, J.; Tong, B.; Cai, Z.; Zhi, J.; Dong, Y. Synthesis of poly(amine-furan-arylene)s through a one-pot catalyst-free *in situ* cyclopolymerization of diisocyanide, dialkylacetylene dicarboxylates and dialdehyde. *Macromolecules* **2019**, *52*, 729–737.
- Mao, L.; Sakurai, H.; Hirao, T. Facile synthesis of 2,3-disubstituted quinoxalines by Suzuki-Miyaura coupling. *Synthesis* **2004**, *15*, 2535–2539.
- Sandmann, B.; Happ, B.; Vitz, J.; Paulus, R. M.; Hager, M. D.; Bartscher, P.; Moszner, N.; Schubert, U. S. Metal-free cycload-



- dition of internal alkynes and multifunctional azides under solvent-free conditions. *Macromol. Chem. Phys.* **2014**, *215*, 1603–1608.
- 30 Song, B.; He, B.; Qin, A.; Tang, B. Z. Direct polymerization of carbon dioxide, diynes, and alkyl dihalides under mild reaction conditions. *Macromolecules* **2018**, *51*, 42–48.
- 31 Wei, B.; Li, W.; Zhao, Z.; Qin, A.; Hu, R.; Tang, B. Z. Metal-free multicomponent tandem polymerizations of alkynes, amines, and formaldehyde toward structure- and sequence-controlled luminescent polyheterocycles. *J. Am. Chem. Soc.* **2017**, *139*, 5075–5084.
- 32 Alizadeh, A.; Rostamnia, S.; Zhu, L. G. Competition of the R3P/DAAD and RNC/DAAD zwitterions in their production and reaction with aromatic carboxylic acids: A novel binucleophilic system for three-component synthesis of 2-aminofurans. *Synthesis* **2008**, *2008*, 1788–1792.
- 33 Urdl, K.; Weiss, S.; Karpa, A.; Perić, M.; Zikulnig-Rusch, E.; Brecht, M.; Kandelbauer, A.; Müller, U.; Kern, W. Furan-functionalised melamine-formaldehyde particles performing Diels-Alder reactions. *Eur. Polym. J.* **2018**, *108*, 225–234.
- 34 Suzuki, Y. Synthesis and characterization of high refractive index and high Abbe's number poly(thioether sulfone)s based on tricyclo[5.2.1.0<sup>2,6</sup>]decane moiety. *Macromolecules* **2012**, *45*, 3402–3408.
- 35 Cai, Z.; Zhang, Y.; Song, Y.; Cheng, Q.; Zheng, Y.; Cui, Z.; Shi, Z.; Chen, C.; Zhang, D. Optically transparent fluorine-containing polycarbonates with high refractive indices for thermo-optic switches. *Mater. Chem. Front.* **2017**, *1*, 2031–2038.
- 36 Faurie, A.; Mallet, C.; Allain, M.; Skene, W. G.; Frère, P. Topological and packing mode modification for solid-state emission enhancement of bis(perfluorostyryl)furan derivatives. *New J. Chem.* **2016**, *40*, 6728–6734.
- 37 Qiu, Z.; Liu, X.; Lam, J. W. Y.; Tang, B. Z. The marriage of aggregation-induced emission with polymer science. *Macromol. Rapid Commun.* **2019**, *40*, 1800568.
- 38 Hu, R.; Xin, D. H.; Qin, A. J.; Tang, B. Z. Polymers with aggregation-induced emission characteristics. *Acta Polymerica Sinica* (in Chinese) **2018**, 132–144.
- 39 Dong, H.; Zhu, H.; Meng, Q.; Gong, X.; Hu, W. Organic photoresponse materials and devices. *Chem. Soc. Rev.* **2012**, *41*, 1754–1808.
- 40 Yildirim, Y. Influence of  $\gamma$ -ray irradiation on the thermal stability and conductivity of polyfuran. *Asian J. Chem.* **2013**, *25*, 7582–7586.
- 41 Christensen, E.; Fioroni, G. M.; Kim, S.; Fouts, L.; Gjersing, E.; Paton, R. S.; McCormick, R. L. Experimental and theoretical study of oxidative stability of alkylated furans used as gasoline blend components. *Fuel* **2018**, *212*, 576–585.